Positron-annihilation studies of rhombic triacontahedral-type icosahedral quasicrystals and their 1/1 and 2/1 approximants in the Al-Mg-Zn alloy system

K. Sato,* H. Uchiyama, Y. Takahashi, and I. Kanazawa
Department of Physics, Tokyo Gakugei University, 4-1-1, Koganei, Tokyo 184-8501, Japan

R. Suzuki and T. Ohdaira
Quantum Radiation Division, Electrotechnical Laboratory, 1-1-4, Umezono, Tsukuba, Ibaraki 305-8568, Japan

T. Takeuchi, T. Mizuno, and U. Mizutani
Department of Crystalline Materials Science, Nagoya University, Nagoya 464-8603, Japan
(Received 18 December 2000; published 13 June 2001)

Rhombic triacontahedral-type icosahedral quasicrystal and its 1/1 and 2/1 approximants in Al-Mg-Zn alloy system were systematically studied by means of positron-annihilation lifetime measurements and positron-annihilation lifetime and Doppler-broadening measurements using the slow-positron-beam technique. We could successfully derive the structural vacancy density in this alloy system. The structural vacancy densities were $\sim 4.56\times10^{-3}$ for the 1/1 approximants, 4.82×10^{-3} for the 1/2 approximant, and 5.05×10^{-3} for the icosahedral quasicrystal. In addition, the positron motions were investigated. The average positron-diffusion length, average positron-diffusion length in matrix, positron-diffusion coefficient, and positron mobility in this alloy system including the icosahedral quasicrystal were estimated. The positron-diffusion coefficients for the 1/1 approximants were almost identical (~ 1.79 cm^2 s^{-1}) to each other, but decrease down to 1.61×10^{-1} cm^2 s^{-1} for the 2/1 approximant and 1.44×10^{-1} cm^2 s^{-1} for the icosahedral quasicrystal. This first experimental estimation was performed by coupling the positron-annihilation lifetime measurements to the positron-annihilation Doppler-broadening measurements using the slow-positron beam excellently. The results indicated that the thermarized positrons in matrix tend to localize as the order of the approximant increases.

DOI: 10.1103/PhysRevB.64.024202 PACS number(s): 61.44.Br, 41.75.Fr, 71.60.+z, 78.70.Bj

I. INTRODUCTION

Since the discovery of icosahedral quasicrystals (QC's),[1] much work has been devoted to clarify their structural nature. In particular, the approach in making full use of the atomic structure of the crystalline approximants has been often employed because of the possession of clusters similar to that found in QC's. Based on the atomic structure of the α-Al-Mn-Si compound determined by Cooper and Robinson,[2] Elser and Henley[3] proposed the atomic cluster in this compound to represent well the atomic cluster in icosahedral Al-Mn-Si QC's. Audier *et al.*[4] have investigated the structure of icosahedral Al-Li-Cu QC on the basis of a modified illustration of the Bergman model.[5] The atomic structure of the lowest-order crystalline approximants, namely, 1/1 approximants, is now fairly well studied by using the Rietveld method.[6–8] This indicates that structural information particularly, the structural vacancy density is experimentally well determined in comparison with that in the QC's.

The Al-Mg-Zn alloy system has received attention from the point of view of electronic properties, band calculations, and thermal stability. Since the valence band near the Fermi level E_F is dominated by sp electrons, various electronic properties are essentially determined by the Fermi-surface–Brillouin-zone interaction. The icosahedral QC in this alloy system had been considered to exist only as a metastable phase. However, Takeuchi and co-workers[9–11] found the 2/1 approximant and stable icosahedral QC at two different compositions in a very narrow composition range. Thanks to their discovery, systematic studies on the electron transport properties and relative stability among the three phases 1/1, 2/1, and QC [Ref. 12] have become possible. Recently, Mizutani *et al.*[7] determined the atomic structure of $Al_xMg_{39.5}Zn_{60.5-x}$ ($20.5\leqslant x\leqslant 50.5$) 1/1 approximants as a function of the Al concentration x by the Rietveld method. They concluded that the center of the two clusters in the body-centered cubic (bcc) lattice, which is called site A, is only 10% occupied by Al atoms for $x=20.5$ and that it becomes essentially vacant when x exceeds 30.

Positron-annihilation measurements are known to provide structural information such as vacancy-type defects and dislocations for any material being independent of the structural periodicity unlike the diffraction method. We have already suggested the existence of a dense distribution of structural vacancy-type sites in many kinds of thermally stable icosahedral QC's such as icosahedral Al-Li-Cu,[13] Al-Pd-Mn,[14] Al-Cu-Fe,[15] and Al-Cu-Ru [Ref. 15] QC's by positron-annihilation lifetime measurements. Recently, we have successfully estimated the structural vacancy densities for icosahedral $Al_{70.7}Pd_{21.34}Re_{7.96}$ and $Al_{71.5}Pd_{20.3}Mn_{8.2}$ under saturation-trapping condition by positron-annihilation Doppler–broadening measurements with the slow-positron beam.[16] In that experiment, we determined a positron-trapping radius from the measured S parameter by slow-positron beam. However, the preparation of a centimeter-sized single-phase sample, which is inevitably needed for the slow-positron beam, was made possible only for the 1/1 approximant in the present Al-Mg-Zn alloy system. Hence, we employed a different approach to determine the structural

vacancy densities for the 2/1 approximant and icosahedral QC as described below.

We have attempted to determine the occupancy of the center site of the RT cluster in $Al_{25.5}Mg_{40}Zn_{25.5}$ 1/1 approximant by using the slow-positron beam. The structural vacancy density for the $Al_{25.5}Mg_{40}Zn_{25.5}$ 1/1 approximant can be calculated by using the occupancy thus obtained. As a next step, the positron specific trapping rate for the center site of the RT cluster was determined by combining with the results of positron-annihilation lifetime measurements. By assuming that 1/1, 2/1 approximants, and icosahedral QC in the Al-Mg-Zn alloy system are constructed by packing the RT cluster, we can estimate the structural vacancy densities by using the positron-specific trapping rate. The structural vacancy densities thus obtained were found to increase, as the order of the approximant increases to the icosahedral QC.

In addition, the positron motion in this alloy system was systematically investigated. It is known that the positron motion provides information about lattice vibrations in solids.[17] The study of positron motion began with the measurements of drift velocities based on the Doppler shift in the annihilation radiation by Mills and Pfeiffer.[18] Simpson *et al.*[19] measured a positron mobility in Si by using the positron-lifetime method. The slow-positron-beam technique has been effectively used to determine the positron-diffusion coefficient in metals and semiconductors for the last few years.[20–22] So far, there exists no reliable measurement of the positron-diffusion constant or the positron mobility in the icosahedral QC. If the icosahedral QC's can be regarded as being intermediate between the crystalline phase and the amorphous phase, the investigation of the positron motion in icosahedral QC's is of great significance. Unfortunately, as described above, since positron-annihilation measurements can detect a dense distribution of structural vacancy, which could not be removed by annealing icosahedral QC, it is difficult to examine the positron motion in the matrix of icosahedral QC. This means that the experimental determination of positron-diffusion coefficient and the positron mobility without being affected by defect interaction is not feasible. In the present experiments, we could obtain the positron lifetimes corresponding to the annihilation in the matrix from the positron-annihilation lifetime method. Hence, the positron motion in the matrix of 1/1, 2/1 approximants, and icosahedral QC in the Al-Mg-Zn alloy system were investigated without being affected by the structural vacancy, by coupling the positron-lifetime method with the slow-positron-beam technique.

In this study, the positron lifetime and slow-positron-beam measurements were performed to determine both the structural vacancy and positron motion in 1/1, 2/1 approximants, and icosahedral QC in the Al-Mg-Zn alloy system. The quantitative values of the structural vacancy density, the average positron-diffusion length, the average positron-diffusion length in the matrix, the positron-diffusion coefficient, and the positron mobility were presented.

II. EXPERIMENT

Alloy ingots were prepared by induction melting of appropriate amounts of constituent elements 99.99% Al, 99.9% Mg, and 99.99% Zn in a boron-nitride crucible under Ar pressurized atmosphere. Ribbon specimens were fabricated by melt spinning onto a copper wheel at a tangential speed of 52 m/s. The icosahedral QC, its 1/1 and 2/1 approximants were heat treated at 573 K for 2 h. The formation of the quasicrystalline single phase and the approximant single phases after thermal treatments was confirmed by x-ray diffraction with Cu Kα radiation. The composition was analyzed for representative samples by using inductively coupled plasma photoemission spectroscopy. It agreed well with the nominal composition within $\pm 1\%$.

The positron-annihilation lifetime measurements were performed for ribbon specimens of icosahedral QC, its 1/1 and 2/1 approximants around room temperature. Ribbon specimens were neatly piled up together enough to stop the fast positrons entirely. The positron-annihilation lifetime spectra were recorded with a fast-fast coincidence system employing a photomultiplier Hamamatsu H2431Q with 1×1 in^2 BaF_2 scintillators. The time resolution of this system was 230 ps full width at the half maximum (FWHM). For each spectrum at least 1.0×10^6 annihilations were counted. The time resolution function was assumed to be composed of two Gaussian functions. Using this time resolution function, the lifetime in the bulk of well-annealed pure Al (purity 99.9999 wt. %) was measured as 166 ± 2 ps. After subtracting the background, positron-annihilation lifetime spectra were analyzed using POSITRONFIT.[23]

The positron-annihilation measurements by slow-positron beam were performed for ingot specimen of the $Al_{25.5}Mg_{39.5}Zn_{35}$ 1/1 approximant at room temperature by use of the positron pulsing system with an intense slow positron beam generated by an electron linac in Electrotechnical Laboratory LINAC facility. The lifetime spectra were obtained by measuring the time interval between the timing signal derived electrically from the pulsing system and the timing signal of an annihilation γ ray detected with BaF_2 scintillation detector. The detailed lifetime-measurement system is described elsewhere.[24] For each spectrum at least 3.0×10^5 counts were accumulated. The positron-annihilation lifetime spectra were analyzed using the ''RESOLUTION'' routine[25] with good variance of the fits with a time resolution if about 290 ps FWHM.

The positron-annihilation Doppler-broadening measurement by slow positron beam was performed for ingot specimen of $Al_{25.5}Mg_{39.5}Zn_{35}$ 1/1–approximant. The experimental setup of the slow-positron beam is composed of ^{22}Na positron source (about 5 mm Ci) and a single W $\langle 100 \rangle$ foil of 1-μm thickness. The foil was annealed at 2273 K in vacuum of $\sim10^{-9}$ Torr, and was attached in front of the source to moderate the positrons. A fraction of these energetic positrons emitted from a ^{22}Na source is thermalized through a variety of collision processes in a tungsten moderator and are reemitted from this moderator as monoenergetic slow positrons. The intensity of the slow-positron beam is about 1.0×10^4/s. The incident positron energy is varied in the range 0–13 keV. The measurements of Doppler-broadening spectra by slow-positron beam were carried out at room temperature by use of a solid-state detector (pure Ge). The total counts in a spectrum corresponding to each incident positron energy

were 8.0×10^4. The data acquisition was repeated eight times for each data point in order to improve the statistical precision.

In order to estimate the vacancy-type defects in the sample, the S parameter was measured. The measured S parameter data were analyzed by using the scaling function.[26–28] When the energy of monoenergetic low-positron beam is reduced to thermal energy k_BT, their spatial distribution $\tilde{P}(E,z)$ in a sample along the incident direction (z) can be described by a scaling function:[26,27]

$$\tilde{P}(E,z)=N_{lm}\left(\frac{u}{C_{lm}}\right)^{l}\exp\left[-\left(\frac{u}{C_{lm}}\right)^{m}\right], \tag{2.1}$$

where N_{lm} is a normalized constant, and C_{lm}, l, and m are parameters, which depend on a material chosen,[27,28] and u is defined as

$$u=\frac{z}{\langle z(E)\rangle}, \tag{2.2}$$

where $\langle z(E)\rangle$ is a mean implantation depth. The mean implantation depth $\langle z(E)\rangle$ is assumed to be given by

$$\langle z(E)\rangle=\frac{A_i}{\rho_i}E^{\alpha_i+\beta_i lnE}, \tag{2.3}$$

where E and ρ_i are the incident energy of the beam and the density of the sample, respectively. From Monte Carlo simulations, the parameters A_i, α_i, and β_i are found to depend on the atomic number of the constituent elements.[29]

After thermalization, positrons begin to diffuse in the sample. The positron diffusion is described by the following diffusion equation in one dimension:

$$D_+\frac{\partial^2N(z,t)}{\partial z^2}-\frac{\partial N(z,t)}{\partial t}-\Gamma N(z,t)=0, \tag{2.4}$$

where D_+ is the positron-diffusion coefficient, $N(z,t)$ is the positron density as a function of both the time and position, and $\Gamma=\lambda_f+\kappa_d$ is the effective annihilation rate of positron, λ_f is the bulk annihilation rate. The observed S parameter is given by a linear combination of contributions from different annihilation sites,

$$S(E)=\sum_i S_iF_i(E), \tag{2.5}$$

where $F_i(E)$ is the fraction of positrons annihilating in the ith state characterized by the S_i parameter and E is the incident energy of the positron beam. The fraction $F_i(E)$ can be obtained by solving the diffusion equation, subjected to the positron implantation profile and boundary conditions. By fitting Eq. (2.5) to the measured S parameter data, one can obtain the average positron-diffusion length L_d,

$$L_d=\sqrt{\frac{D_+}{\lambda_f+\kappa_d}}, \tag{2.6}$$

at a given temperature.

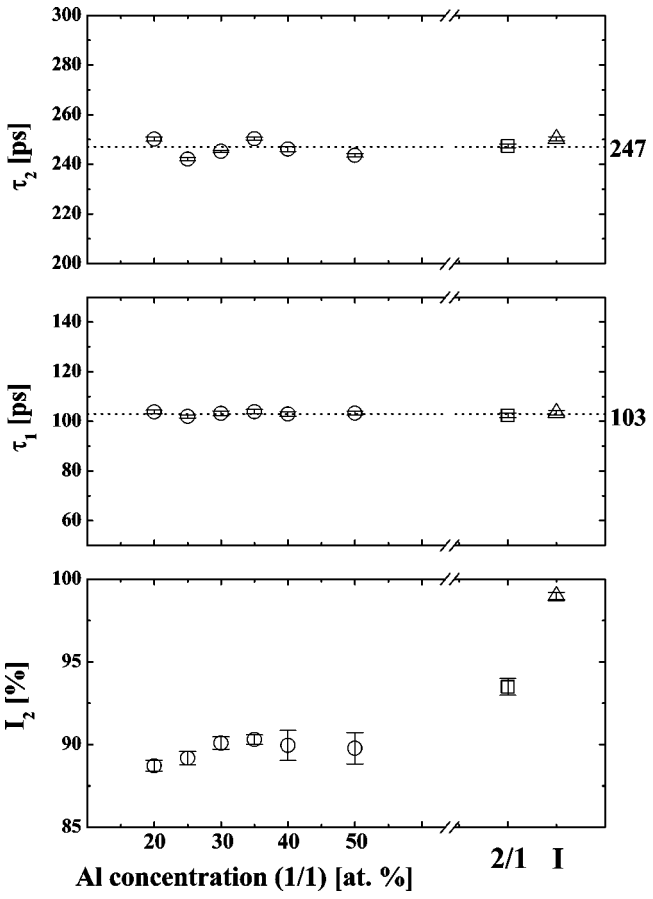

FIG. 1. Electron-concentration dependence of the positron-annihilation lifetimes for the $Al_xMg_{39.5}Zn_{60.5-x}$ ($20.5\leqslant x\leqslant 50.5$) 1/1 approximants (open circles), the $Al_{15}Mg_{43}Zn_{42}$ 2/1 approximant (open squares), and the icosahedral $Al_{15}Mg_{44}Zn_{41}$ QC (open triangles).

III. RESULTS AND DISCUSSION

The observed lifetime spectra of the $Al_xMg_{39.5}Zn_{60.5-x}$ ($20.5\leqslant x\leqslant 50.5$) 1/1 approximants, the $Al_{15}Mg_{43}Zn_{42}$ 2/1 approximant, and the icosahedral $Al_{15}Mg_{44}Zn_{41}$ QC were analyzed in terms of two components with the lifetimes τ_1 and τ_2. Figure 1 shows the lifetimes τ_1 and τ_2 together with the relative intensity I_2 of τ_2 ($I_1=1-I_2$) as a function of Al concentration for the $Al_xMg_{39.5}Zn_{60.5-x}$ ($20.5\leqslant x\leqslant 50.5$) 1/1 approximants, the $Al_{15}Mg_{43}Zn_{42}$ 2/1 approximant, and the icosahedral $Al_{15}Mg_{44}Zn_{41}$ QC. The lifetimes τ_1 and τ_2 for the $Al_xMg_{39.5}Zn_{60.5-x}$ ($20.5\leqslant x\leqslant 50.5$) 1/1 approximants are found to be essentially independent of the Al concentration and are centered at 103 ps and 247 ps, respectively. The relative intensities I_2 for 1/1 approximants are approximately 90% in the whole range. We attributed the lifetimes τ_1 and τ_2 to the annihilation at the bulk and vacancy-type defect, respectively. In the present system, the cluster center of the bcc lattice sites is most likely the candidate for the vacancy-type defects.

The values of the lifetimes τ_1 and τ_2 for the $Al_{15}Mg_{43}Zn_{42}$ 2/1 approximant and icosahedral $Al_{15}Mg_{44}Zn_{41}$ QC are found to be essentially identical to these for a series of the 1/1 approximants. This means that

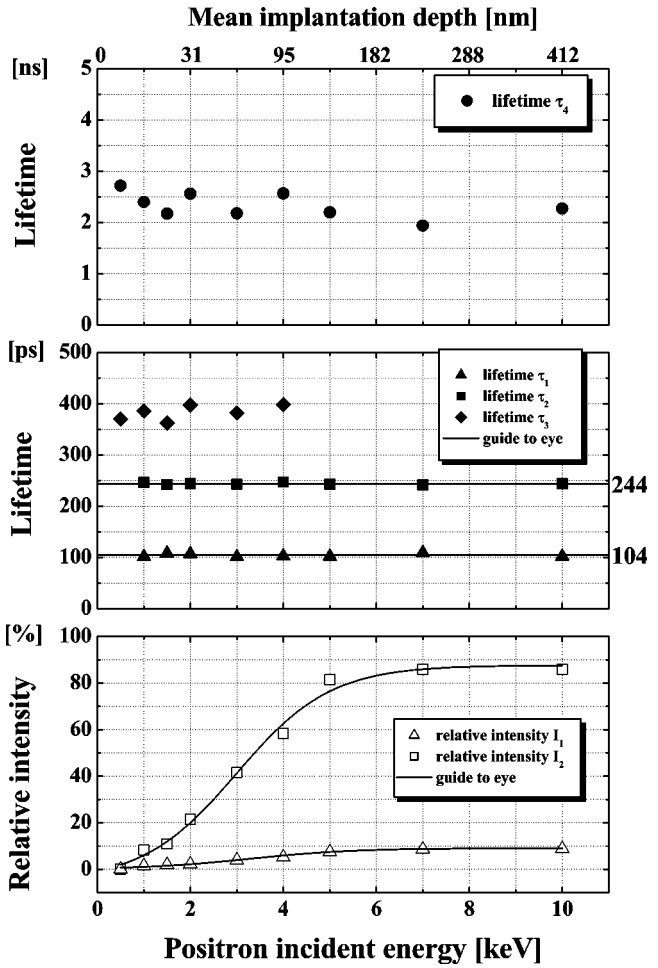

FIG. 2. Positron-annihilation lifetimes and relative intensities for the $Al_{25.5}Mg_{39.5}Zn_{35}$ 1/1 approximant as a function of the positron-incident energy. The closed triangles, squares, diamonds, and circles, and open triangles, and squares show the positron-annihilation lifetimes τ_1, τ_2, τ_3, and τ_4 and the relative intensities I_1 and I_1. The solid lines are guides to the eye.

there is no significant difference in the vacant sites in the cluster among the three phases. In other words, the vacant site in 2/1 approximant and icosahedral QC exists at the center of the RT cluster. The relative intensity I_2 for the 2/1 approximant is $\sim$93%, which is apparently high in comparison with the series of the 1/1 approximants. More remarkable is the relative intensity I_2 ($\sim$99%) for the icosahedral QC, which is much higher than that for the 2/1 approximant. This means that the vacant site apparently increases as the order of the approximant increases to the icosahedral QC.

Next, we have measured the change of the positron-annihilation lifetime in the $Al_{25.5}Mg_{39.5}Zn_{35}$ 1/1 approximant by using the slow-positron beam of variable energies. The obtained lifetime spectra were well fitted with three or four lifetime components. Figure 2 shows the lifetimes τ_1, τ_2, τ_3, and τ_4, together with relative intensities I_1 of τ_1 and I_2 of τ_2 at the positron incident energies 0.5, 1, 1.5, 2, 3, 4, 5, 7, and 10 keV. The values of the lifetimes τ_3 and τ_4 are in the range from 350 ps to 450 ps and from 1 ns to 4 ns, respectively. We attributed lifetimes τ_3 and τ_4 to the annihilations

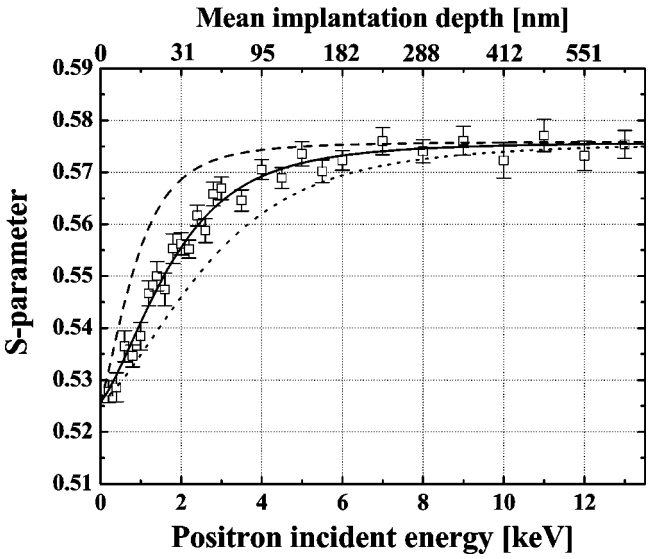

FIG. 3. *S* parameter for the $Al_{25.5}Mg_{39.5}Zn_{35}$ 1/1 approximant as a function of the positron incident energy. Statistical errorbars for the absolute accuracy are shown. The solid line is a result of a weighted nonlinear fit, in which the r_d and p_A were determined 3.1 Å and 63%, respectively. The dotted and dashed lines represent the results of calculation assuming the structures derived from Bergman *et al.* (Ref. 5) and Mizutani *et al.* (Ref. 7), respectively.

of the *ortho*-positronium (o-Ps) trapped at a surface state and its pick-off annihilation on the surface, respectively. The lifetimes τ_1 and τ_2 were observed the positron-incident energy of above 1.0 keV. These values are centered at 104 ps and 244 ps, and are consistently identical in the whole energy range. These agree closely with the lifetimes τ_1 and τ_2 obtained from the conventional positron-annihilation measurements. Hence, we attributed these lifetimes τ_1 and τ_2 to the annihilations at the bulk and the vacancy-type defect alike the conventional positron-annihilation measurements. The relative intensity I_1 increases slightly and becomes $\sim$9% at 10 keV. The relative intensity I_2 increases gradually and becomes $\sim$86% at 10 keV. These values of the relative intensities I_1 and I_2 also agree with the conventional positron-annihilation measurements. This means that the result by the slow-positron beam is consistent with the one by the conventional positron-annihilation lifetime measurements.

We have also measured the *S* parameter for the $Al_{25.5}Mg_{39.5}Zn_{35}$ 1/1 approximant by using the slow-positron beam as a function of the positron-incident energy. The results are shown in Fig. 3 (open squares). The value of the measured *S* parameter increases, but is saturated above about 7 keV. From the analysis of the measured *S*-parameter data, we can derive the occupancy p_A of the site *A* and the positron-trapping radius r_d as follows. The probability P_n, in which a positron diffuses through the *n* unit cells without being trapped at the site *A*, is given by

$$P_n = \left[1 - \frac{8\pi r_d^3 (1-p_A)}{3l^3} \right]^n , \qquad (3.1)$$

where a is the lattice constant of the unit cell, i.e., 14.16 Å. The positron-diffusion length L is, therefore, equal to

$$L = an. \tag{3.2}$$

The probability P_n is rewritten as

$$P_n = \left[1 - \frac{8\pi r_d^3 (1 - p_A)}{3l^3} \right]^{L/a}. \tag{3.3}$$

In Eq. (3.3), the value of L such that P_n is decayed $1/e$ times the initial value, is an average positron-diffusion length. Hence, in the process of diffusion of positron to the surface, the average positron-diffusion length in the $Al_{25.5}Mg_{39.5}Zn_{35}$ 1/1 approximant can be expressed as a function of the trapping radius r_d and the occupancy p_A of the site A. Since we found the positron-annihilation lifetime spectra of the $Al_{25.5}Mg_{39.5}Zn_{35}$ 1/1 approximant to be composed of nearly a single component, Eq. (2.5) can be written as

$$S = S_s F_s + S_d F_d, \tag{3.4}$$

where S_s and S_d are the values of the S parameter for surface and structural vacant sites, and F_s and F_d $(=1-F_s)$ are the annihilation rate for surface and structural vacant sites, respectively. The determination of the two parameters (r_d, p_A) in Eq. (3.3) was made by using the weighted nonlinear least-square method. A solid line in Fig. 3 gives the result of a fit, in which r_d and p_A were determined to be 3.1 Å and 63%, respectively. Provided that the site A at the cluster center is only vacant site existing in the 1/1 approximant, we are led to conclusion that the site A is 63% occupied. The present value of the occupancy for the site A is different from $p_A = 80\%$ obtained by Bergman *et al.*,[5] and $p_A = 0\%$ obtained by Mizutani *et al.*[7] The dotted and dashed lines in Fig. 3 represent the results of the calculation by assuming the structures derived from Bergman *et al.*[5] and Mizutani *et al.*,[7] respectively.

The structural vacancy density C_d for the $Al_{25.5}Mg_{39.5}Zn_{35}$ 1/1 approximant is deduced to be 4.57×10^{-3}. The positron-trapping rate κ_d is calculated as 5.06×10^9 s^{-1} from the relation

$$\kappa_d = \frac{1}{\tau_1} \left(1 - \frac{I_1 \tau_2 + I_2 \tau_1}{\tau_2} \right), \tag{3.5}$$

by using the measured values of τ_1, τ_2, I_1, and I_2 of the conventional positron-annihilation lifetime measurement. Hence, the specific-positron trapping rate ν_d for the site A turns out to be 1.11×10^{12} s^{-1} from the relation

$$\nu_d = \frac{C_d}{\kappa_d}. \tag{3.6}$$

Since τ_1 and τ_2 are essentially same for the three phases, we can reasonably assume that there exists no difference in the density of the site A among the three phases. This means that the value of positron-specific trapping rate ν_d is also the same for the three components. Since the positron-trapping rates κ_d for the $Al_{15}Mg_{43}Zn_{42}$ 2/1 approximant and icosahedral $Al_{15}Mg_{44}Zn_{41}$ QC can be obtained to be 5.35×10^9 and 5.61×10^9 s^{-1} from the conventional positron-annihilation lifetime measurements, the structural vacancy densities C_d for $Al_{15}Mg_{43}Zn_{42}$ 2/1 approximant and icosahedral $Al_{15}Mg_{44}Zn_{41}$ QC are calculated, as listed in Table I. Table I also lists the structural vacancy density C_d for remaining 1/1 approximants, together with that for $Al_{25.5}Mg_{39.5}Zn_{35}$ 1/1 approximant.

TABLE I. The structural vacancy densities for $Al_xMg_{39.5}Zn_{60.5-x}$ 1/1 approximant, $Al_{15}Mg_{43}Zn_{42}$ 2/1 approximant, and icosahedral $Al_{15}Mg_{44}Zn_{41}$ QC.

Phase	Alloy	Structural vacancy density $[10^{-3}]$
1/1 approximant	$Al_{20.5}Mg_{39.5}Zn_{40}$	4.50 ± 0.14
	$Al_{25.5}Mg_{39.5}Zn_{35}$	4.57 ± 0.12
	$Al_{30.5}Mg_{39.5}Zn_{30}$	4.59 ± 0.15
	$Al_{35.5}Mg_{39.5}Zn_{25}$	4.58 ± 0.15
	$Al_{40.5}Mg_{39.5}Zn_{20}$	4.57 ± 0.15
	$Al_{50.5}Mg_{39.5}Zn_{10}$	4.55 ± 0.15
2/1 approximant	$Al_{15}Mg_{43}Zn_{42}$	4.82 ± 0.16
i phase	$Al_{15}Mg_{44}Zn_{41}$	5.05 ± 0.17

We consider the obtained structural vacancy densities C_d through the positron mobility. The obtained structural vacancy densities C_d for icosahedral QC and two different approximants are too high in view of a lower limit (order of 10^{-4}) (Ref. 30) for vacancy density in the typical metals to saturate the positron trapping. This drives us to the question why all thermalized positrons were not trapped into the vacant sites. The positron-annihilation lifetime spectra ought to be composed of a single component, namely, saturation trapping. We mentioned that Eq. (2.5) can be used to obtain the average diffusion length L_d in the sample by fitting Eq. (2.5) to the measured S-parameter data. From fitting to the measured S-parameter data in Fig. 3, an average diffusion length L_d in the $Al_{25.5}Mg_{39.5}Zn_{35}$ 1/1 approximant was determined as 428 Å. As taken from Eq. (2.6), the average diffusion length L_d decreases as the structural vacancy density C_d increases. It can be said that the obtained average diffusion length L_d of 428 Å shortens due to the structural vacancy density C_d of 4.58×10^{-3}. Since the positron-annihilation rate λ_f is obtained to be 4.74×10^9 s^{-1} through the relation

$$\lambda_f = \frac{I_1 \tau_2 + I_2 \tau_1}{\tau_1 \tau_2} \tag{3.7}$$

by using the result of conventional positron-annihilation measurement, a positron-diffusion coefficient D_+ is calculated as 1.80×10^{-1} $cm^2\,s^{-1}$ from Eq. (2.6). The average diffusion length in the matrix L_m $(L_m = \sqrt{D_+/\lambda_f})$ in the $Al_{25.5}Mg_{39.5}Zn_{35}$ 1/1 approximant is estimated to be 616 Å. The average diffusion length in the matrix of 616 Å is considered to be perfectly independent of the structural vacancy. The positron mobility μ_+ at 300 K could be estimated as 6.96 $cm^2\,V^{-1}\,s^{-1}$ via the Einstein relation

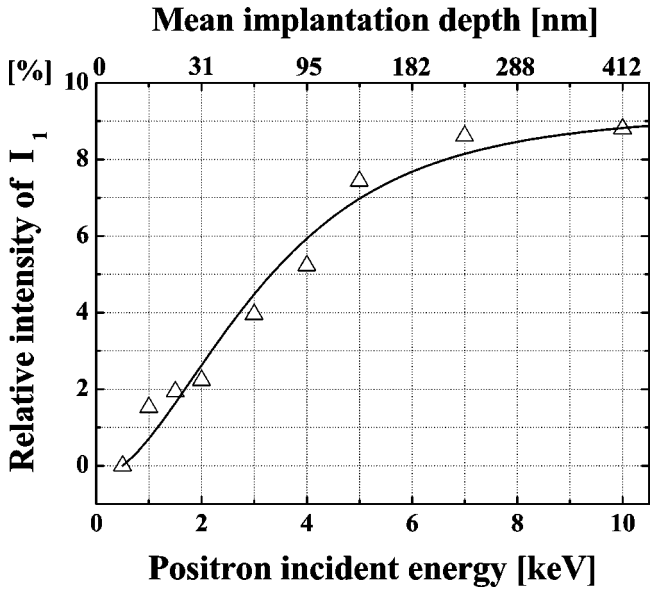

FIG. 4. The measured relative intensity I_1 (open triangles) and calculated one (solid line) for the $Al_{25.5}Mg_{39.5}Zn_{35}$ 1/1 approximant as a function of the positron-incident energy. The calculation was made with the average positron-diffusion length in the matrix L_m of 616 Å.

$$D_+ = \mu_+ \frac{kT}{e}, \tag{3.8}$$

where *k*, *T*, and *e* are the Boltzmann constant, temperature, and an elementary charge, respectively.

In order to ascertain the validity of the average diffusion length in the matrix L_m obtained from the method above, we estimated the average diffusion length in the matrix L_m in a different method. As already mentioned, the relative intensity I_1 shown in Fig. 2 increases slightly. This slight increase can be explained by the positron-annihilation rate in the vicinity of the surface, resulting from the fraction of positrons that return by the average diffusion length in the matrix L_m from the bulk. By taking account of the distributions from the mean implantation depth $\langle z(E) \rangle$ defined by Eq. (2.3), we calculated the theoretical curve of the relative intensity I_1 as a function of the positron-incident energy. Figure 4 shows the measured relative intensity I_1 (open triangles) and calculated one (solid line), with the average diffusion length in the matrix, L_m, of 616 Å. It should be noticed that the value of 616 Å is in an excellent agreement with the value obtained from above method. This leads support to the derivation of the average diffusion length in the matrix L_m obtained from the diffusion coefficient D_+.

The obtained values of the positron-diffusion coefficient D_+, the positron-diffusion length L_m, and mobility μ_+ are lower than those for typical metals by an order of magnitude. Positron-diffusion coefficient D_+ in several cubic metals was studied by Soininen *et al.*,[20] and turned out to be $1-2$ $cm^2\,s^{-1}$. Also band-structure calculations for most metals yield approximately $D_+ \approx 1$ $cm^2\,s^{-1}$ at room temperature.[31] We concluded that the thermalized positrons could not diffuse sufficiently in the matrix of the $Al_{25.5}Mg_{39.5}Zn_{35}$ 1/1 approximant. Namely, the positrons of $\sim 10\%$ remain in the matrix before reaching the vacant site and are annihilated there without being trapped into the vacant site. The reason why few percents of positrons were not trapped into the vacant site can be equally applied to remaining 1/1 approximants, 2/1 approximant, and icosahedral QC.

Finally, we estimated the average positron-diffusion length L_m in the matrix of the $Al_{15}Mg_{43}Zn_{42}$ 2/1 approximant and icosahedral $Al_{15}Mg_{44}Zn_{41}$ QC. We have already mentioned that the obtained structural vacancy densities C_d of these two compounds are 5.35×10^{-3} and 5.61×10^{-3}. Here, we assume that the structure of the $Al_{15}Mg_{43}Zn_{42}$ 2/1 approximant and icosahedral $Al_{15}Mg_{44}Zn_{41}$ QC are composed of the bcc packing of the RT cluster with respective C_d, whose the lattice constant is 14.16 Å. Then, the values of the occupancy p_A of the site *A* for the $Al_{15}Mg_{43}Zn_{42}$ 2/1 approximant and icosahedral $Al_{15}Mg_{44}Zn_{41}$ QC can be calculated as 61% and 59%. In both cases, the value of the positron-trapping radius r_d of 3.1 Å was used. The average positron-diffusion lengths L_d are thus calculated as 406 Å and 387 Å by using above occupancies p_A and positron-trapping radii r_d. The positron-diffusion coefficient D_+ and average diffusion length in matrix L_m are derived by following the same procedure as that for the $Al_{25.5}Mg_{39.5}Zn_{35}$ 1/1 approximant. The values of the positron-diffusion coefficient D_+ for the 1/1 approximants are almost identical (~ 1.79 $cm^2\,s^{-1}$) to each other, but decrease down to 1.61×10^{-1} $cm^2\,s^{-1}$ for the 2/1 approximant and 1.44×10^{-1} $cm^2\,s^{-1}$ for the icosahedral QC. From Eq. (3.8), positron mobilities μ_+ in the $Al_{15}Mg_{43}Zn_{42}$ 2/1 approximant and icosahedral $Al_{15}Mg_{44}Zn_{41}$ QC at 300 K are estimated as 6.23 and 5.57 $cm^2\,V^{-1}\,s^{-1}$, respectively. Table II summarizes L_d, L_m, D_+, and μ_+ for the $Al_{25.5}Mg_{39.5}Zn_{35}$ 1/1, and $Al_{15}Mg_{43}Zn_{42}$ 2/1 approximant, icosahedral $Al_{15}Mg_{44}Zn_{41}$ QC, and the remaining 1/1 approximants. The error bars in these values were calculated based on the law of error propagation in the calculation process. From Table II, we can immediately see a feature that the thermarized positrons in the matrix become less diffusive as the order of the approximant increases.

Since the first positron experiment on amorphous or glassy alloys by Chen and Chaung,[32] a center of interest has focused on the strong localization of positrons in these alloys. Kong *et al.*[33] measured a very small positron mobility of 13×10^{-3} $cm^2\,V^{-1}\,s^{-1}$ in amorphous SiO_2. The significant positron trapping by unidentified sites has been reported in some of these alloys,[34,35] whereas the existence of vacancy-type defects has been excluded.[36,37] We could estimate the positron diffusion coefficient D_+ of 1.44×10^{-1} $cm^2\,s^{-1}$ and the positron mobility μ_+ of 5.57 $cm^2\,V^{-1}\,s^{-1}$ for icosahedral QC without being affected by the structural vacancy. From the results of the positron-annihilation lifetime measurement, it is hardly conceivable that positrons are trapped at regions such as the effective free volume, a low electron-density area, the dislocation, the interface, and the grain boundary, except for the structural vacancy. If the icosahedral QC's are characterized as being intermediate between the crystals and glasses, it

TABLE II. The average positron-diffusion lengths, average positron-diffusion lengths in matrix, positron-diffusion coefficients, and positron mobilities for $Al_xMg_{39.5}Zn_{60.5-x}$ 1/1 approximant, and $Al_{15}Mg_{43}Zn_{42}$ 2/1 approximant and icosahedral $Al_{15}Mg_{44}Zn_{41}$ QC. L_d, L_m, D_+, and μ_+ are the average positron-diffusion length, average positron-diffusion length in matrix, positron-diffusion coefficient, and positron mobility, respectively.

Phase	x	L_d (Å)	L_m (Å)	D_+ (10^{-1} $cm^2\,s^{-1}$)	μ_+ ($cm^2V^{-1}\,s^{-1}$)
1/1	20.5	434±12	627±17	1.82±0.10	7.04±0.39
	25.5	428±12	616±17	1.80±0.10	6.96±0.39
	30.5	426±12	618±17	1.77±0.10	6.85±0.39
	35.5	427±12	622±18	1.76±0.10	6.81±0.39
	40.5	428±12	620±17	1.78±0.10	6.89±0.39
	50.5	430±12	621±17	1.80±0.10	6.96±0.39
2/1		406±11	603±17	1.61±0.09	6.23±0.35
I		387±11	597±17	1.44±0.08	5.57±0.31

might be said that the localization of positron wave function is due to the destruction of the translational symmetry in icosahedral QC.

IV. CONCLUSIONS

Rhombic triacontahedral-type icosahedral quasicrystal and its 1/1 and 2/1 approximants in the Al-Mg-Zn alloy system were systematically studied by means of positron-annihilation experiments. We revealed the structural vacancy densities in 1/1, 2/1 approximants, and icosahedral QC in Al-Mg-Zn alloy system. The obtained structural vacancy densities increased as the order of the approximant increased to the icosahedral QC. The positron motion in this alloy system was also investigated. We presented the average positron-diffusion length, average positron-diffusion length in matrix, average positron-diffusion coefficient, and positron mobility in this alloy system including icosahedral QC. These values show that the thermarized positrons in matrix are not easy to diffuse as the order of the approximant increases. The annihilations in the bulk of a few percent of positrons are considered to be due to the difficulty to diffuse.

ACKNOWLEDGMENTS

K.S. and I.K. would like to thank Professor H. Murakami and Professor M. Nakata, Tokyo Gakugei University, for helpful suggestions and comments.

*Present address: Department of Applied Physics, University of Tokyo, Hongo, Bunkyo-ku, Tokyo 113-8656, Japan.

[1] D. Shechtman, I. Blech, D. Gratias, and J.W. Cahn, Phys. Rev. Lett. **259**, 53 (1984).
[2] M. Cooper and K. Robinson, Acta Crystallogr. **20**, 614 (1966).
[3] V. Elser and C.L. Henley, Phys. Rev. Lett. **55**, 2883 (1985).
[4] M. Audier, P. Sainfort, and B. Dubost, Philos. Mag. Lett. **54**, 105 (1986).
[5] G. Bergman, J.L.T. Waugh, and L. Pauling, Acta Crystallogr. **10**, 254 (1957).
[6] U. Mizutani, W. Iwakami, and T. Fujiwara, in *Proceedings of the 6th International Conference on Quasicrystals*, edited by S. Takeuchi and T. Fujiwara (World Scientific, Singapore, 1997), pp. 579–582.
[7] U. Mizutani, W. Iwakami, T. Takeuchi, M. Sakata, and M. Takata, Philos. Mag. Lett. **76**, 349 (1997).
[8] W.J. Kim, P.C. Gibbons, K.F. Kelton, and W.B. Yelon, Phys. Rev. B **58**, 2578 (1998).
[9] T. Takeuchi, S. Murasaki, A. Matsumoto, and U. Mizutani, J. Non-Cryst. Solids **156–158**, 914 (1993).
[10] U. Mizutani, T. Takeuchi, and T. Fukunaga, Mater. Sci., JIM **34**, 102 (1993).
[11] T. Takeuchi, Y. Yamada, T. Fukunaga, and U. Mizutani, Mater. Sci. Eng., A **181–182**, 828 (1994).
[12] T. Takeuchi and U. Mizutani, Phys. Rev. B **52**, 9300 (1995).
[13] T. Ohata, I. Kanazawa, T. Iwashita, K. Kishi, and S. Takeuchi, Phys. Rev. B **42**, 6730 (1990).
[14] I. Kanazawa, E. Hamada, T. Saeki, K. Sato, M. Nakata, S. Takeuchi, and M. Wollgarten, Phys. Rev. Lett. **79**, 2269 (1997).
[15] E. Hamada, N. Oshima, T. Suzuki, K. Sato, I. Kanazawa, M. Nakata, and S. Takeuchi, Mater. Sci. Forum **255–257**, 451 (1997).
[16] K. Sato, Y. Takahashi, H. Uchiyama, I. Kanazawa, R. Tamura, K. Kimura, F. Komori, R. Suzuki, T. Ohdaira, and S. Takeuchi, Phys. Rev. B **59**, 6712 (1999).
[17] *Positron Solid State Physics*, edited by W. Brandt and A. Dunpasquier (North-Holland, Amsterdam, 1983).
[18] A.P. Mills, Jr. and L. Pfeiffer, Phys. Rev. Lett. **36**, 1389 (1976).
[19] R.J. Simpson, M.G. Stewart, C.D. Beling, and M. Charlton, J. Phys.: Condens. Matter **1**, 7251 (1989).
[20] E. Soininen, H. Huomo, P.A. Huttunen, J. Mäkinen, A. Vehanen, and P. Hautojärvi, Phys. Rev. B **41**, 6227 (1990).
[21] J. Mäkinen, C. Corbel, P. Hautojärvi, and D. Mathiot, Phys. Rev. B **43**, 12 114 (1991).
[22] Y.Y. Shan, K.G. Lynn, P. Asoka-Kumar, S. Fung, and C.D. Beling, Phys. Rev. B **55**, 9897 (1997).
[23] P. Kirkegaard and M. Eldrup, Comput. Phys. Commun. **7**, 401 (1974).
[24] R. Suzuki, Y. Kobayashi, T. Mikado, H. Ohgaki, M. Chiwaki, T. Yamazaki, and T. Tomimasu, Jpn. J. Appl. Phys., Part 2 **30**, L532 (1991).

[25] P. Kirkegaad, M. Eldrup, O.E. Mogensen, and N.J. Pedersen, Comput. Phys. Commun. **23**, 237 (1981).
[26] V.J. Ghosh, D.O. Welch, and K.G. Lynn, in *Proceedings of the 5th International Workshop on Slow Positron Beams for Solids and Surface*, edited by E. H. Ottewitte (AIP, New York, 1992), p. 937.
[27] V.J. Ghosh, Appl. Surf. Sci. **85**, 187 (1995).
[28] G.C. Aers, P.A. Marshall, T.C. Leung, and R.D. Goldberg, Appl. Surf. Sci. **85**, 196 (1995).
[29] G.C. Aers, J. Appl. Phys. **76**, 1622 (1994).
[30] R.M. Nieminen and M. Manninen, *Positrons in Solids*, Topics in Current Physics Vol. 12 (Springer-Verlag, Berlin, 1979), p. 145.
[31] O.V. Boev, M.J. Puska, and R.M. Nieminen, Phys. Rev. B **36**, 7786 (1987).
[32] H.S. Chen and S.Y. Chuang, Phys. Status Solidi A **25**, 581 (1974).
[33] Y. Kong, T.C. Leung, P. Asoka Kumar, B. Nielsen, and K.G. Lynn, J. Appl. Phys. **70**, 2874 (1991).
[34] E. Cartier and F. Heinrich, Helv. Phys. Acta **53**, 266 (1980).
[35] Z. Kajcsos, S. Mantl, W. Triftshäuser, and J. Winter, Phys. Status Solidi A **58**, 77 (1980).
[36] H.S. Chen and S.Y. Chuang, J. Electron. Mater. **4**, 783 (1975).
[37] S. Tanigawa, K. Hinode, R. Nagai, K. Kanbe, M. Doyama, and N. Shiotani, Phys. Status Solidi A **51**, 249 (1979).